

# Multi-Constellation GNSS Multipath Mitigation Using Consistency Checking

Ziyi Jiang, Paul D Groves  
*University College London, United Kingdom*

Washington Y Ochieng, Shaojun Feng, Carl D Milner  
*Imperial College London, United Kingdom*

Philip G Mattos  
*ST Microelectronics, United Kingdom*

## BIOGRAPHY

Dr Ziyi Jiang is a research fellow at University College London (UCL), currently specialising in multipath mitigation research in the Space Geodesy and Navigation Laboratory (SGNL). He completed his PhD at UCL on digital route model aided integrated satellite navigation and low-cost inertial sensors for high-performance positioning on the railways. He also holds a BEng in measuring and control technology from Harbin Engineering University, China ([ziyi.jiang@ucl.ac.uk](mailto:ziyi.jiang@ucl.ac.uk)).

Dr Paul Groves is a Lecturer (academic faculty member) at UCL, where he leads a program of navigation and positioning research within SGNL. He was a navigation systems researcher at QinetiQ from 1997 to 2009. He is interested in all aspects of navigation and positioning, including multi-sensor integrated navigation, robust GNSS under challenging reception conditions, and novel positioning techniques. He is an author of about 40 technical publications, including the book *Principles of GNSS, Inertial and Multi-Sensor Integrated Navigation Systems*. He holds a BA/MA and a DPhil in physics from the University of Oxford. He is a Fellow of the Royal Institute of Navigation and an associate editor of both *Navigation: Journal of the ION* and *IEEE Transactions on Aerospace and Electronic Systems* ([p.groves@ucl.ac.uk](mailto:p.groves@ucl.ac.uk)).

Professor Washington Ochieng holds the Chair in Positioning and Navigation Systems in the Department of Civil and Environmental Engineering at Imperial College London. He is also the Director of the ICEGG and the Departmental Master of Science programmes. He is a Fellow and Member of Council of the Royal Institute of Navigation, and Member of the US Institute of Navigation.

Dr. Shaojun Feng is a Research Fellow at the Centre for Transport Studies within the Department of Civil and Environmental Engineering at Imperial College London. He leads the navigation research team within the Imperial College Engineering Geomatic Group (ICEGG). He is a Fellow of Royal Institute of Navigation and a member of the US Institute of Navigation.

Dr. Carl Milner is a research associate at the Centre for Transport in the Civil and Environmental Engineering Department at Imperial College London. He completed his MMath in Mathematics from the University of Warwick in 2004 before following a young graduate trainee programme in navigation at the European Space Agency (ESA). He gained his doctorate from Imperial College London in 2009.

Professor Philip G Mattos gained Bachelors and Masters degrees in Electronic Engineering from Cambridge, followed by Masters Degrees in Telecoms and Computer Science from Essex in 1977. He joined INMOS in 1979. INMOS was acquired by STMicroelectronics in 1989. He was made a Visiting Research Fellow at Bristol University, and awarded an external PhD on his GPS work in 1996. Since 1989 he has worked exclusively on GPS implementations, and the associated RF front ends. He is now working on system level integrations of GPS, and on the Galileo system, while consulting on the next generation GNSS chips, including one-chip GPS (RF+digital), and high sensitivity GPS and Galileo for indoor applications, and combined GPS/Galileo/Glonass chipsets. In 2008/9 he re-implemented LORAN on the GPS CPU, and in 2009/2010 led the GLONASS implementation team. He has recently been appointed a visiting professor at the University of Westminster.

## ABSTRACT

In a typical urban environment, a mixture of multipath-free, multipath-contaminated and non-line-of-sight (NLOS) propagated GNSS signals are received. The errors caused by multipath-contaminated and NLOS reception are the dominant source of reduced consumer-grade positioning accuracy in the urban environment. Many conventional receiver-based and antenna-based techniques have been developed to mitigate either multipath or NLOS reception with mixed success. Nevertheless, the positioning accuracy can be maximised based on the simple principle of selecting only those signals least contaminated by multipath and NLOS propagation to form the navigation solution. The advent of multi-constellation GNSS provides the opportunity to realise this technique that is potentially low-cost and effective for consumer-grade devices. It may also be implemented as an augmentation to other multipath mitigation techniques.

The focus of this paper is signal selection by consistency checking, whereby measurements from different satellites are compared with each other to identify the NLOS and most multipath-contaminated signals. The principle of consistency checking is that multipath-contaminated and NLOS measurements produce a less consistent navigation solution than multipath-free measurements. RAIM-based fault detection operates on the same principle.

Three consistency-checking schemes based on single-epoch least-squares residuals are assessed: single sweep, recursive checking and a hybrid version of the first two. Two types of weighting schemes are also considered: satellite elevation-based and signal  $C/N_0$ -based weighting. The paper also discussed the different observables that may be used by a consistency-checking algorithm for different applications and their effect on detection sensitivity.

Test results for the proposed algorithms are presented using data from both static positioning and stand-alone dynamic positioning experiments. The static data was collected using a pair of survey-grade multi-constellation GNSS receivers using both GPS and GLONASS signals at open sky and urban canyon locations, while the dynamic data was collected using a consumer-grade GPS/GLONASS receiver on a car in a mixed urban environment. Significant improvements in position domain are demonstrated using the weighted recursive methods in the open environments. However in the urban environments, there are insufficient directly received signals for the conventional RAIM-based signal selection to be effective all the time. Both positioning improvements and risky outliers are demonstrated. More advanced techniques have been identified for investigation in future research.

## 1. INTRODUCTION

Conventional multipath mitigation methods [1, 2] are mostly based on the assumption that only a single GNSS constellation is used. However, multi-constellation GNSS provides access to many more signals. Accuracy can thus be maximised by selecting only those signals least contaminated by multipath and NLOS propagation to form the navigation solution and discarding the rest. With single-constellation GNSS, there is limited scope to do this without compromising the availability of a position solution with adequate geometry, particularly in challenging environments, such as city centres.

For consumer-grade positioning applications in cities, single frequency receivers are mostly used and the positioning solutions are commonly produced from the code-based pseudorange measurements. Although the multipath effect affects both code- and carrier-phase observations, code-phase multipath is on a much larger scale and is usually the dominant error source for urban positioning situations. Diffracted and reflected signals can easily result in ten-meter-order positioning errors when only basic single-epoch positioning algorithms are applied. In extreme but not uncommon cases, where NLOS signals are tracked, hundreds of meters of positioning error can be present without further checking mechanisms.

The advent of multi-constellation GNSS thus provides the opportunity for a new approach to multipath mitigation, applicable to most environments. Both single-epoch least-squares-based and multiple-epoch Kalman filter-based positioning algorithms can benefit from the application of signal selection. A number of different techniques, including dual-polarization antennas [3], may be used for detecting multipath-contaminated and/or NLOS signals. However, no single method is effective at identifying all of these signals.

The focus of this paper is signal selection by consistency checking, whereby measurements from different satellites are compared with each other to identify the NLOS and multipath-contaminated signals. Consistency checking does not require additional equipment or a database and does not make the assumption of a single specular reflector. It can operate using only one measurement per satellite, though sensitivity is improved by using multiple measurements. It may thus be used either as a low-cost alternative to the other methods or as an augmentation to improve overall robustness.

The principle of consistency checking is that multipath-contaminated and NLOS measurements produce a less consistent navigation solution than multipath-free measurements. In other words, if position solutions are computed using combinations of signals from different

satellites, those obtained using only the multipath-free signals should be in greater agreement than those that include multipath-contaminated and NLOS measurements. Thus these measurements may be identified through various consistency-checking based approaches, such as residual outlier detection from an all-satellite least-squares solution. By eliminating these contaminated measurements, a more accurate position solution can be produced. The same principle is used for fault detection in receiver autonomous integrity monitoring (RAIM) [4, 5]. The difference is that, in RAIM, the object is to detect and exclude faulty data and to calculate protection levels, whereas here, the aim is to identify the set of measurements least affected by multipath and NLOS propagation.

The performance of the consistency-checking algorithm depends on the type of ranging observable used. Here, a ranging observable is defined as any combination of GNSS pseudo-range, pseudo-range rate and/or carrier phase measurement from single or multiple epochs, single or multiple frequencies, single or multiple satellites and single or multiple receivers. An optimal observable would combine signals such that nuisance elements, such as atmospheric effects and satellite clock errors, are excluded, while sensitivity to multipath and NLOS errors is maximised. Section 2 discusses the suitability of different observables for use in different applications and their likely sensitivity. Factors to consider include the receiver design, whether the application is static or dynamic, and the positioning mode (differential or stand-alone). Further observables that enable the consistency checking to be weighted are also discussed.

Section 3 describes three consistency-checking algorithms based on least-squares residual outlier detection. The first method detects outliers in a single sweep method, where all measurement residuals are compared against a threshold and the all residuals that exceed the threshold are removed. The second approach is based on recursive RAIM. A recursive RAIM-like statistical test is carried out on the set of normalised residuals. The largest normalised residual is eliminated and a new least-square solution computed with the remaining measurements until the statistical test is passed. The third method is a hybrid of the other two.

Section 4 presents the test results using three sets of data include two static scenarios and a car navigation scenario. The data used covers environments from open sky to severe urban canyon situations. Significant positioning improvements are demonstrated with the open sky data set using the weighted recursive method. Improvements are also demonstrated in the urban area, but some environments were shown to be too challenging for the current version of the consistency checking techniques.

Finally Section 5 summarises the conclusions and presents plans for future works.

## **2. OBSERVABLES FOR CONSISTENCY CHECKING BASED MULTIPATH MITIGATION**

The performance of a consistency-checking algorithm depends on the type of observables used, i.e. the data that is input to the algorithm. Two categories of observable are considered here: ranging observables and weighting observables. For each satellite whose measurements are considered for inclusion in the navigation solution, there is one ranging observable. However there may be more than one weighting observable or none.

The ranging observables are what the algorithm compares with each other in order to determine their consistency. These may be any combination of GNSS pseudo-range, pseudo-range rate and/or carrier phase measurement from single or multiple epochs, single or multiple frequencies, single or multiple satellites and single or multiple receivers. It can also include corrections from an ionospheric and/or tropospheric model. The ranging observable used for consistency checking doesn't have to be the same as the one used to calculate the navigation solution.

The weighting observables provide a prior indication of the likelihood that measurements from a given satellite are multipath-contaminated and/or NLOS. They may be used to bias the consistency-checking algorithm by applying different weightings to the ranging observables that are compared with each other. Weighting observables should be constructed using different information from the ranging observables.

An optimal observable of either type would combine signals such that nuisance elements, such as atmospheric effects and satellite clock errors, are minimised, while sensitivity to multipath and NLOS errors is maximised. Ranging observables will also depend on the geometric range from satellite(s) to receiver(s) and on the receiver clock error(s); weighting observables will not. The information available to construct such observables depends on the application. The ranging observable is considered first.

The worst case is single-frequency stand-alone static GNSS user equipment. Here, the residual ionosphere and troposphere propagation errors are of a similar size to typical code multipath errors, potentially greater in some cases. Furthermore, the medium-delay multipath, which tends to produce the largest pseudo-range errors, varies relatively slowly. For applications, such as many location-based services, where a quick fix is required, the pseudo-range may be the only viable ranging observable. In this case, consistency checking may only highlight the NLOS

errors, which are typically much larger than multipath errors.

Sensitivity to multipath and NLOS errors is significantly enhanced where better calibration of the ionosphere error, typically the largest bias-like error, is achievable, either using a dual-frequency receiver or differential GNSS. Dual-frequency operation typically removes more of the ionosphere error. However differential GNSS can also reduce the ephemeris and satellite clock errors and, in local area implementations, the troposphere error, further improving the sensitivity to multipath of consistency checking.

For applications where dual user equipment in close proximity may be installed, differencing the two sets of measurements will essentially eliminate the ionosphere, troposphere, satellite clock and ephemeris errors completely, leaving a ranging observable that depends only on multipath and NLOS errors, tracking errors, and the difference in geometric range and receiver clock. This observable will be highly sensitive to multipath, significantly enhancing the effectiveness of consistency checking. However, the hardware costs will be doubled unless relative positioning is required anyway.

For applications, such as surveying, where data may be collected for several minutes at one location, a multipath-sensitive ranging observable may be constructed by applying frequency-dependent filtering. Low-pass filtering will reduce the impact of ionosphere, troposphere, ephemeris and satellite clock errors, while high-pass filtering and/or carrier-smoothing of the pseudo-ranges, will significantly reduce the tracking errors. The multipath and NLOS errors will typically vary at an intermediate frequency.

For dynamic applications, the multipath and NLOS errors vary rapidly with time as the path delay of the reflected signals changes. This renders the multipath errors much easier to distinguish from the slower varying errors. Consequently, a multipath- and NLOS-sensitive ranging observable may be constructed by time-differencing the pseudo-range measurements.

A comparison of these different types of ranging observable and the optimisation of the relevant tuning parameters is a subject for future research. The results presented here are derived using conventional single-frequency pseudo-range-based observables. Carrier smoothing is applied in the static scenarios, but not the dynamic scenario. In both cases, the broadcast satellite clock corrections, Klobuchar ionosphere model and MOPS troposphere model [7] are used.

Moving on to the weighting observables, it is common practice to apply higher weighting to signals from high-

elevation satellites on the principle that these typically exhibit lower multipath errors. However, they also exhibit lower ionosphere and troposphere errors.

The carrier-power-to-noise density,  $C/N_0$ , may also be used as a weighting observable as NLOS signals are typically attenuated on reflection. A more sophisticated observable may be constructed by comparing the left-hand and right-hand circularly polarised  $C/N_0$  measurements from a dual-polarisation antenna [3].

A further observable may be constructed for road and rail applications by comparing the azimuth of the satellite signal with the host vehicle trajectory. This is because there are typically fewer buildings and other obstructions along the direction of travel than perpendicular to it.

A highly multipath-sensitive weighting observable for dynamic applications may be constructed from the receiver's correlator outputs, or  $I_s$  and  $Q_s$ . Because the reflected signals always arrive after the direct signals, they will particularly distort the late correlator measurements with little effect on the early correlators. This distortion can be positive or negative, depending on whether the reflected signals are in-phase or anti-phase with the direct signal. This results in a highly variable amplitude for the late correlator, while the early correlator is much less affected. However looking at the late correlator alone is not sufficient, as similar variations will occur due to variable attenuation, as in passing trees etc. These variations will affect both early and late amplitudes simultaneously. Consequently, a multipath-sensitive observable may be constructed by maintaining a normalised variance of the amplitude over (short) time periods for the early, and separately, the late correlators, and comparing these [6].

The results presented here consider the use of elevation and  $C/N_0$  as weighting observables.

### 3. CONSISTENCY CHECKING ALGORITHMS FOR MULTIPATH MITIGATION

A fault detection and exclusion algorithm such as RAIM is designed based on the principle that a faulty signal would be less consistent to normal signals, either in the measurement or the solution domain. The underlying assumptions of RAIM consistency checking are:

- Measurement errors follow a zero-mean Gaussian distribution;
- Faulty signals are the minority amongst the received signals; and
- The errors on different signals are independent of each other.

Based on these assumptions the RAIM consistency checking tries to answer two hypothesis-testing questions:

does a failure exist? and, if so, which is the failed satellite? [8]

Multipath-contaminated and NLOS signals tend to be inconsistent with “clean” signals. This inconsistency, however, differs depending on the degree of the contamination. The scale of multipath and NLOS error introduced on the code-phase pseudorange measurement in an urban environment implies a more severe inconsistency than in an open field. While RAIM is designed to identify inconsistency caused by faults in the received signals, the consistency checking methods can be applied to identify contaminated signals.

Various schemes have been developed to implement RAIM. The differences among different schemes are mainly focused on different ways to separate the faulty signals [1] and whether the consistency checking is carried out on a single-epoch snapshot basis [4] or by a filtering approach [8].

The snapshot-based approach attributes not only a faster response to sudden inconsistencies, but also the advantage of avoiding questionable assumptions about how a system arrives at its current state [4]. Hence the snapshot-based approach is more prevalent than the filtering approach. The consistency-checking algorithm developed in this research is on a snapshot basis.

Two very important parameters involved in the consistency-checking process are the testing statistics and the decision threshold. Common methods to calculate the testing statistics include range comparison, least-squares residuals and parity methods. Since all three methods are conceptually the same and produce similar results, the least-squares-residuals method is chosen for this work because of the simplicity of implementation. The decision threshold, on the other hand, respects the basic assumptions of consistency checking about the measurement error distribution, and follows a chi-square distribution.

A RAIM-type consistency-checking algorithm is firstly introduced in Section 3.1. Three different implementation schemes are explained in Section 3.2. Two weighting scheme, based on satellite elevation and signal C/N<sub>0</sub>, are described last in Section 3.3. The treatment for a combined GPS/GLONASS least-squares solutions is presented in Section 3.4.

### 3.1 CONSISTENCY CHECKING ALGORITHM

The basic measurement and solution relationship can be described by an over-determined system of linear equations in the form of (assuming  $n$  measurements are available,  $m$  unknowns need to be determined, and  $n \geq m$ )

$$\tilde{\mathbf{y}} = \mathbf{G}\mathbf{x} + \mathbf{e} \quad (1)$$

where  $\tilde{\mathbf{y}}$  is a  $n \times 1$  measurement vector accommodating the differences between the actual measured pseudorange and the predicted ranges based on the nominal user position;  $\mathbf{x}$  is a  $m \times 1$  state vector containing the solution needed;  $\mathbf{G}$  is a  $n \times m$  measurement matrix describing the linear connection between the measurement vector  $\tilde{\mathbf{y}}$  and the state vector  $\mathbf{x}$ ; And  $\mathbf{e}$  is the measurement error vector ( $n \times 1$ ) which is a combination of all ranging errors such as residual satellite orbit and clock, residual atmospheric effects and multipath etc.

The well-known least-squares solution of the problems stated in Equation (1) can be written as [8]

$$\hat{\mathbf{x}} = (\mathbf{G}^T \mathbf{G})^{-1} \mathbf{G}^T \tilde{\mathbf{y}} \quad (2)$$

where  $\hat{\mathbf{x}}$  is the least-squares solution. A  $n \times 1$  residual vector  $\mathbf{w}$  can be calculated using a predicted measurement vector  $\hat{\mathbf{y}}$ , which can be calculated with

$$\hat{\mathbf{y}} = \mathbf{G}\hat{\mathbf{x}} \quad (3)$$

Hence the residual vector  $\mathbf{w}$  is obtained by

$$\mathbf{w} = \tilde{\mathbf{y}} - \hat{\mathbf{y}} = [\mathbf{I} - \mathbf{G}(\mathbf{G}^T \mathbf{G})^{-1} \mathbf{G}^T] \tilde{\mathbf{y}} \quad (4)$$

The test statistic used for the testing is based on the sum of the squared errors (SSE), which is defined as [8]

$$\text{SSE} = \mathbf{w}^T \mathbf{w} \quad (5)$$

and the test statistic is

$$\text{teststatistic} = \sqrt{\text{SSE}/(n-m)} \quad (6)$$

The determination of the test threshold  $T$  requires a normalised chi-squared distribution threshold  $T_{chi}$ , which can be calculated using a suitable confidence level and the degrees of freedom (DOF). The DOF is the dependence of the estimated parameters on the available measurements. In this case there are  $n-m$  DOF. The test threshold can then be decided using

$$T = \sigma \sqrt{T_{chi} / (n-m)} \quad (7)$$

where  $\sigma$  is an assumed standard deviation of the measurement error depending on the positioning environment.

The decision process of the consistency checking can be presented by a hypothesis-testing problem:

- The null hypothesis  $H_0$  – No inconsistency occurred among measurements.
  - The alternative hypothesis  $H_1$  – inconsistency occurred among measurement.
- and is implemented by comparing the test statistics against the threshold, if:
- test statistics  $\leq T$ ,  $H_0$  is accepted.
  - test statistics  $> T$ ,  $H_1$  is accepted.

The measurements used in this process can be any of the ranging observables as discussed in Section 2.

### 3.2 IMPLEMENTATION SCHEMES

Three different testing schemes are proposed here to implement the consistency checking as described. The main difference among the three schemes is whether the least-squares solution is recalculated at intermediate stages. Different testing thresholds could be applied to accommodate individual testing schemes.

With all methods, there is a risk of eliminating too many measurements, resulting in inadequate position solution geometry. Therefore, for applications where solution availability is most important, measurement elimination should cease at the stage where best accuracy is predicted. Conversely, where accuracy and/or integrity are more important, the position solution should be rejected where they are not achievable.

#### Single Sweep

A brief illustration of the single sweep process is shown in Figure 1. The least-squares solution is firstly computed when the checking begins, and the normalised measurement residuals are used to compute the test statistics. If the test is passed, i.e. no inconsistency is found under the test criteria, all measurements are kept. Otherwise the measurement with the largest normalised residual is eliminated. New test statistics and threshold are then calculated to continue the test. A new solution is calculated with the remaining measurements once the test is passed or the minimum number of measurements remain.

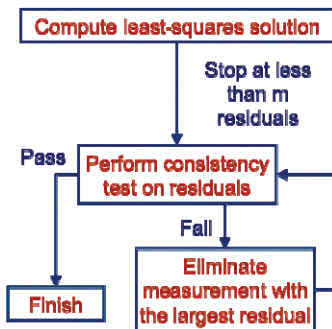


Figure 1: The single sweep scheme

#### Recursive Checking

A brief illustration of the recursive checking process is shown in Figure 2. The least-squares solution is firstly computed as the starting point of the checking. A test statistic is calculated using the measurement residuals. The result of the comparison between the test statistics and the threshold indicates whether an inconsistency is identified among the available measurements. A failed test result will lead to the elimination of the measurement with the largest normalised residual. Unlike the single sweep scheme, a new least-squares solution is recomputed after each elimination, hence producing a new set of residuals. The test statistics and the threshold are all recomputed with the new residuals. This recursive procedure carries on until the test is passed, or insufficient measurements remain.

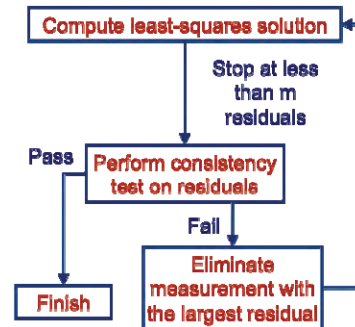


Figure 2: The recursive-checking scheme

#### Hybrid Scheme

A hybrid scheme is a combination of the single sweep and recursive-checking schemes. The checking process at each epoch is performed in two stages, and different thresholds are set up for different stages. The single sweep is firstly carried out with a higher threshold. The remaining measurements from the first stage are then checked under a lower threshold using the recursive method. This is more computationally efficient than recursive checking but less so than the single-sweep method.

### 3.3 WEIGHTING SCHEMES

As discussed in Section 3.2, different weighting scheme could be applied to the measurements during the least-squares calculation. Two weighting methods, respectively based on satellite elevation angles and signal C/N<sub>0</sub>, are considered in this paper.

When applying the weight matrix  $\mathbf{W} (n \times n)$ , the estimated state vector in Equation (2) becomes:

$$\hat{\mathbf{x}} = (\mathbf{G}^T \mathbf{W} \mathbf{G})^{-1} \mathbf{G}^T \mathbf{W} \tilde{\mathbf{y}} \quad (8)$$

$\mathbf{W}$  is defined as

$$\mathbf{W} = \text{diag}(\sigma_1^2, \dots, \sigma_j^2, \dots, \sigma_n^2)^{-1} \quad (9)$$

where  $\sigma_j$  is the modelled standard deviation of each measurement. The difference between the two weighting schemes lies in the modelling of  $\sigma_j$ .

### Elevation Angles

The principle of elevation-angle-based weighting is the assumption that signals with higher elevation are less likely to be affected by errors occurred during the propagation. The model used to form  $\sigma_j$  in this research is described by [7]:

$$\sigma_j = a + b \cdot \exp(-\text{elev}_j / 10) \quad (10)$$

where  $a$  and  $b$  are model parameters. Various models could be used to generate the weight. Other popular forms include the usage of sin- and cos-based atmospheric delay mapping functions. The differences between various models are beyond the scope of this paper.

### Signal C/N<sub>0</sub>

The signal C/N<sub>0</sub> is an effective indication of the received signal strength, which is normally lower for reflected signals. The model used to form  $\sigma_j$  using measured C/N<sub>0</sub> in this research is described by [9]:

$$\sigma_j^2 = c \cdot 10^{-\frac{C/N_{0j}}{10}} \quad (11)$$

where  $c$  is the model parameter. Although antenna and receiver designs can affect the absolute C/N<sub>0</sub> value, the relative comparison of C/N<sub>0</sub> among received signals can still indicate the quality of received signals.

## 3.4 COMBINED GPS/GLONASS SOLUTIONS

The conventional model for a corrected GPS pseudorange measurement is described by [10]:

$$\tilde{\rho}_G = r + c_{light} \cdot \delta t_u + \tilde{\epsilon}_G \quad (12)$$

where  $\tilde{\rho}_G$  is the corrected GPS pseudorange measurement after the troposphere and ionosphere corrections have been applied to the measured ranges;  $r$  is the true geometry range between the satellite at the signal emission time and the receiver at the signal reception time;  $c_{light}$  is the speed of light;  $\delta t_u$  is the receiver clock bias relative to GPS time at the signal reception time; and

$\tilde{\epsilon}_G$  consists of residuals after applying corrections from navigation data and other unmodeled errors. Four unknowns are present in Equation (12) including the receiver coordinates and the receiver clock bias.

A modelling for a corrected GLONASS pseudorange measurement, however, must take into account the time frame difference between GPS and GLONASS system time. For a dual-constellation solution, where the number of measurement available is greatly increased (as shown in Section 4), this time frame different can be treated as an extra unknown  $\delta t_{G-R}$ . Hence Equation (12) for GLONASS measurements becomes

$$\tilde{\rho}_R = r + c_{light} \cdot (\delta t_u + \delta t_{G-R}) + \tilde{\epsilon}_R \quad (13)$$

Note that a minimum of 5 GPS and GLONASS measurements are needed because of the extra unknown parameter.

Both Equation (12) and (13) are incorporated into the linear system described by Equation (1) to solve for the receiver position.

## 4. TEST RESULTS AND DISCUSSION

Multiple tests were conducted for the assessment of the consistency checking algorithms. Three sets of data were used covering both static and dynamic situations. All data sets are collected in London representing various typical urban positioning environments. In all three scenarios, both GPS and GLONASS signals were collected in order to explore the full capacity of the algorithm when more than one constellation is available.

The first two data sets were collected using a Leica Viva GS15 GNSS receiver, shown in Figure 3. The last data set was collected with a prototype GPS/GLONASS receiver developed by ST Microelectronics.

Truth references were provided for each data set to compare against the processing results from the new algorithm. The truth references for the first two data sets are both accurate to cm-level, and the truth references for the last data set is a filtered and map-matched solution which is accurate to meter-level. A pair of Leica System 500 receivers and a total station was used in the process of setting up the truth reference for the second data set.

Test results are presented in this section. All solutions from all three data sets are determined using a positioning algorithm based on single-epoch weighted least squares as described in Section 3.1.



**Figure 3:** Leica Viva GS15 GNSS receiver

#### 4.1 SCENARIO 1: OPEN ROOF

##### Data collection

This set of data is collected on the roof of a UCL building in central London. The data collection was carried out on 20th April 2011. The occupied location is the highest point among neighbouring blocks. The site has a clear view of the sky and is surrounded only by a few scattered obstructions including higher buildings from several blocks away and some existing roof structures, as shown in Figure 4. The set up of the experiment is shown in Figure 5. The data was collected at a 1Hz rate for 5 hours.



**Figure 4:** Site view for Scenario 1 data collection



**Figure 5:** Receiver set up for Scenario 1 data collection

The collected data is post-processed against observations from Ordnance Survey reference stations around London using Real Time Kinematic (RTK) to provide an averaged solution with cm-level accuracy. This solution is used as the truth for this test scenario.

The satellite visibility during the data collection period is shown in Figure 6. The average number of satellites

available is 18, the number of GPS satellites available is 10 and the number of GLONASS satellites available is 8.

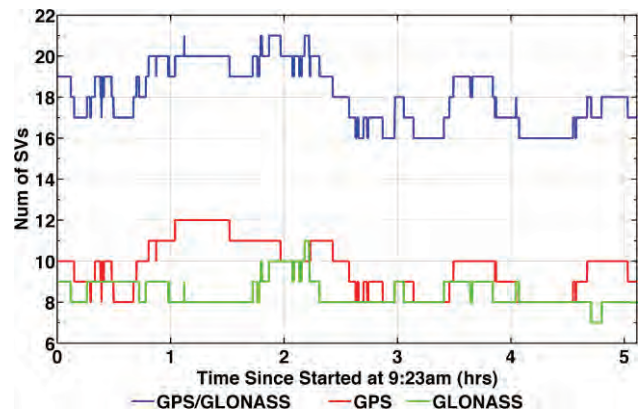


**Figure 6:** Satellite visibility during the data collection in Scenario 1

##### Different Consistency Checking Schemes

All three proposed consistency-checking schemes were tested with the same one-hour data set starting from 10AM. The L1 carrier-smoothed pseudorange measurements were used for all schemes. The weighting scheme was based on satellite elevations. All positioning errors were computed by comparing against the RTK processing results, and the errors for solutions not using any checking schemes are also show for reference. Comparison results are shown in Figure 7 and Table 1.

As can be seen from the RMS errors shown in Table 1, the recursive checking scheme provides the most performance improvement among all proposed schemes, the positioning errors of which improve from 2.56m in easting, 5.2m in northing and 4.65m in height to 1.07m in easting, 1.03m in northing and 1.06m in height. On the other hand, as shown in Figure 7, the single sweep scheme fails to provide a stable improvement; it sometimes deteriorates the performance.

During the tested period, the single sweep scheme exhibited a highly unstable performance. This indicates the checking cannot always correctly identify the multipath contaminated signals. This can be explained by the fact that there is usually more than one contaminated signal and they all have different degrees of contamination. The presence of multiple multipath contaminated signals causes all measurement residuals to be biased. Although the most inconsistent signals can be very easily identified and eliminated, any further elimination on the remaining signal become risky because less contaminated signals are indistinguishable from the biased residuals. Furthermore, because only the biased residuals are available, the single sweep scheme shows greater sensitivity to the checking threshold set-up to other schemes, requires a higher threshold to avoid the

situation where too many satellites are falsely eliminated and the system can only use minimum number of the required measurements that are left.

The recursive-checking scheme, on the other hand, minimises the impact of the biased residuals by recalculating the solution after each elimination. The new residuals are a better representation of the new position fix and can show the updated inconsistency information among the remaining signals. Hence it is possible for the recursive scheme to apply a lower testing threshold than the single sweep scheme. During the test period, the recursive-checking scheme worked more effectively with a lower threshold. As can be seen from Figure 7, the systematic biases in the positioning errors presented in the solutions without any checking are greatly reduced after applying the recursive scheme. Since multipath errors are considered the dominant systematic errors, the results indicate an effective reduction in the multipath contamination. However, a lower threshold could present problems when all signals are heavily contaminated by multipath and NLOS signals are present, taking the urban canyon as an example. A lower threshold could easily let the system eliminate too many satellites and lead to a performance deterioration.

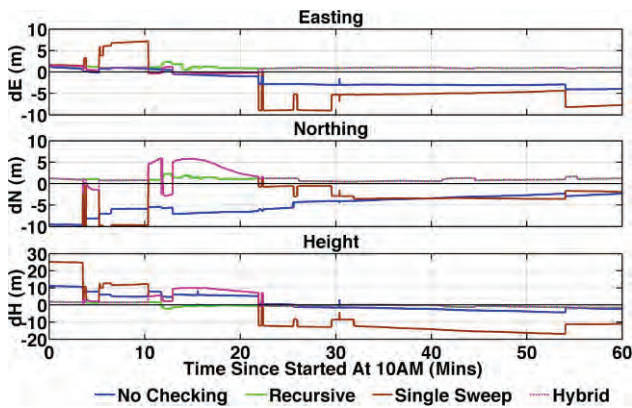


Figure 7: Error comparison for all checking schemes in Scenario 1

	No Checking	Single Sweep	Recursive	Hybrid
Easting	2.56	5.48	1.07	0.92
Northing	5.2	4.97	1.03	2.08
Height	4.65	13.36	1.06	3.76

Table 1: RMS error (Meters) for all checking schemes in Scenario 1

Although slightly better performance improvement can be achieved in certain directions, such as the 0.92m RMS easting errors versus the 1.07m errors from a recursive scheme, the hybrid scheme in general shows poorer performance than the recursive-checking scheme. The superior performance improvement from using a hybrid scheme in the easting direction indicates the importance

of threshold set-up for both checking stages of the scheme. When multiple biases are present, the single sweep method, although less effective because of the biased residuals, can provide a better starting selection of signals for the recursive checking. This suggests an adaptive mechanism for determining the thresholds could be useful, a subject for future research.

Both the recursive and hybrid schemes show performance improvements in a moderate multipath environment such as this scenario, whereas the single sweep scheme is proved to be too sensitive to the presence of multiple contaminated signals.

### Different Weighting Schemes

Two different weighting schemes, based on elevation and C/N<sub>0</sub>, together with the situation when no weighting was applied, were tested with the same one-hour data set starting from 12am. The L1 carrier-smoothed pseudorange measurements were used for all schemes. The recursive consistency checking was applied for all weighting schemes. All positioning errors were computed by comparing against the RTK processing results. A comparison of these positioning errors is shown in Figure 8 and Table 2.

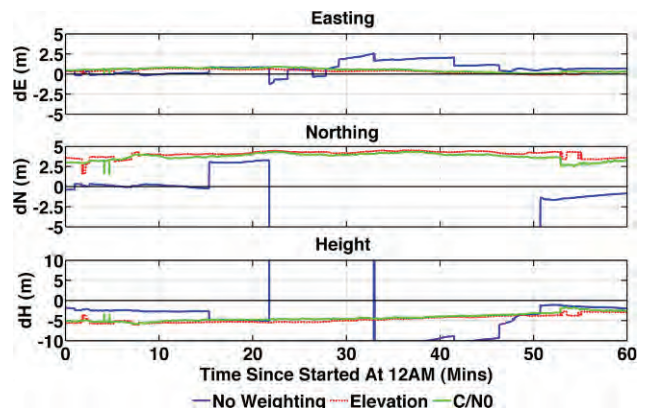


Figure 8: Error Comparison for all weighting schemes in Scenario 1

	No weighting	Elevation	C/N <sub>0</sub>
Easting	1.05	0.42	0.57
Northing	22.49	4.09	3.76
Height	18.76	4.74	4.32

Table 2: RMS error (Meters) for all weighting schemes in Scenario 1

As shown in Table 2, the performance is always improved when a weighting scheme is applied. However, there is no significant difference in the performances of the two weighting schemes.

From Figure 8, it can be observed that the no-weighting solution is more unstable comparing to the other two solutions. For the first 15min of the testing period, the no-weighting solution on both northing and height directions actually out-performed the other two solutions. For the next 40min period, the error for the no-weighting solution, however, increases dramatically, and it is only stable in one direction for a certain period.

This pattern indicates the sensitivity of the consistency-checking scheme when no weighting information is available in a medium multipath environment such as in this scenario. The first-15min no-weighting solution shows great reduction in the systematic bias, which suggests successful selection of consistent signals. The variation of the error directions in the following period, nevertheless, also suggests unsuccessful selection of signals. The inclusion of the different multipath-contaminated signals could cause this shift of direction in the positioning error.

The performances of both weighting schemes, though similar, demonstrates the constraining effect of a weighting scheme when applying consistency checking on signals. Both satellite elevation and signal C/N<sub>0</sub> are additional information to the already biased solutions residuals, as discussed in Section 2.

#### 4.2 SCENARIO 2: CITY CANYON

##### Data collection

This set of data was collected near Moorgate underground station on 8th April 2011. The location for the data collection is within the London City area, where high buildings can easily block the majority of the sky and a lot of glass-surfaced modern buildings, which are much more reflective than brick walls, are situated along the road, as shown in Figure 9. This data represents an urban canyon where severe multipath and signal blocking occurs.



Figure 9: An overview of the data collection location T9

An overview of the locations is shown in Figure 9. The location was occupied for 30 minutes. Figure 10 shows a picture of the set-up of the receiver and the surrounding

environment at the location, T9 (T for previous total station occupation points).



Figure 10: The receiver set-up at the location T9

The truth reference used for this data set was established through traditional surveying methods using total stations and traversing techniques. The reference points of the traversing were set up at a nearby open square where a clear view of the sky is available. GPS data collected with a pair of Leica System 500 receiver was processed using RTK to provide the coordinates for the reference points. The traversing accuracy is 1 in 56000, which is equivalent to cm-level.

The satellite visibility during the data collection period is shown in Figure 11 (results at points T2, T3 and T4 are not presented here). While the average number of satellite available was around 8, it can be seen from Figure 11 that the number of satellites for a single constellation could easily drop below the minimum required for a least-squares solution. A reduced number of available satellites also reduces the probability of simultaneous access to L1 and L2 measurements. Hence a smoothed ionosphere correction [1] is preferable should iono-free ranging observables be tested.

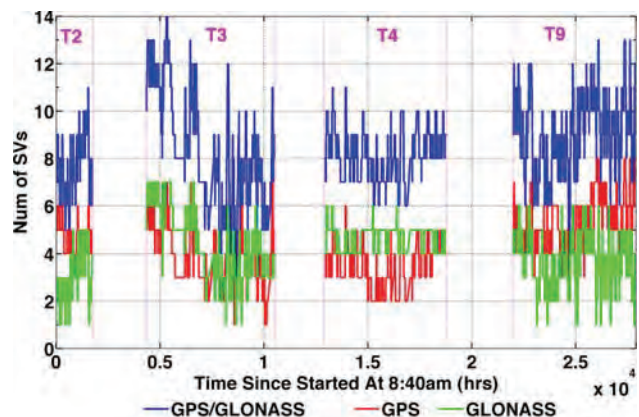


Figure 11: Satellite visibility during the data collection in Scenario 2

##### Different Weighting Schemes

The effect of applying two weighting schemes without using the consistency-checking algorithm is firstly discussed. The test was performed with parts of the data collected at T9. The L1 carrier-smoothed pseudorange observable was used for the test. No consistency-checking scheme was applied. The solution was purely based on the weighted least-squares process. A comparison of the positioning results is presented in Figure 12 and Table 3.

As can be seen from the test results, while no significant performance improvement can be seen after applying the elevation-based weighting, a small reduction of the positioning error can be observed by applying the  $C/N_0$  weighting.

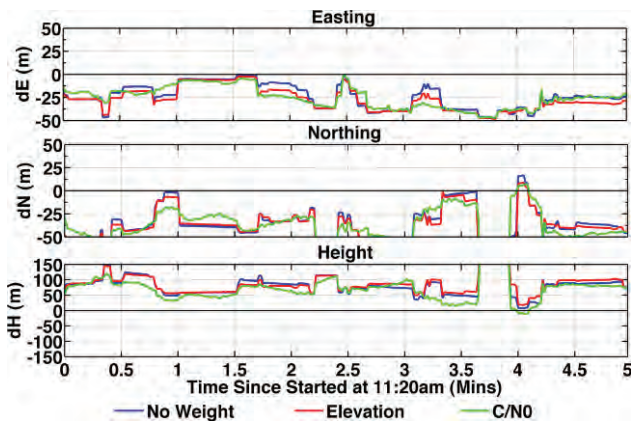


Figure 12: Error Comparison for all weighting schemes without consistency checking in Scenario 2

	No weighting	Elevation	$C/N_0$
Easting	27.49	29.74	28
Northing	52.2	52.37	49.65
Height	97.5	99.92	86.97

Table 3: RMS error (Meters) for all weighting schemes without consistency checking in Scenario 2

### Applying Consistency Checking

Among the three proposed consistency checking schemes, because of the high residual level for all available signals and the reduced number of satellites available (Figure 11), the single sweep and hybrid schemes were fragile at the particularly challenging locations in this data set. Therefore, no results are presented for them. For city environments, the ranging error caused by multipath and NLOS signals affects the majority of received signals. Due to the existence of a large amount of highly reflective objects, the characteristics of these ranging errors also varies quickly with time. As a result, the assumption for the hypothesis testing on which the consistency checking is based breakdown. When only a pre-set fixed threshold is available, only the recursive scheme remains robust, whereas other schemes can easily be forced to a stop

because insufficient signals remain. This suggests further research on constructing a dynamic threshold.

The same data from T9 as used in the weighting schemes test is used here with the recursive-checking scheme. Three sets of results are presented in Figure 13 and Table 4, for which no weighting, elevation-based weighting and  $C/N_0$  weighting are respectively applied.

As can be seen from the results, a performance improvement of about a factor of 2 was achieved by the combined usage of recursive checking and  $C/N_0$  weighting. Figure 14 shows the positioning results and truth reference on a map. As pointed out in Section 4.1, for the consistency checking to work more effectively, additional information is needed. The consistency checking by itself can improve the precision of the solution. But for city positioning scenarios, where precision and accuracy can be quite different, extra observables such as the  $C/N_0$  of individual signals can help to improve the overall accuracy.

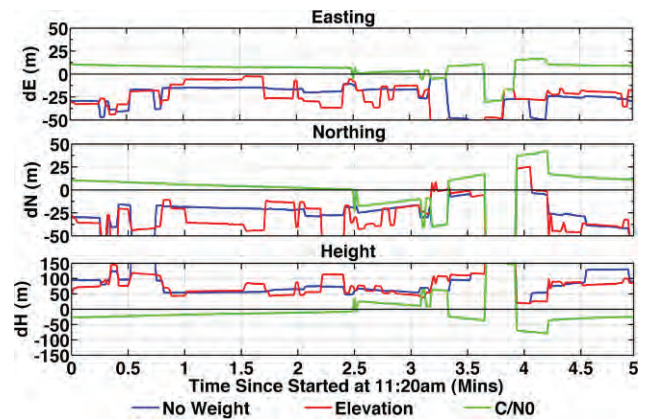
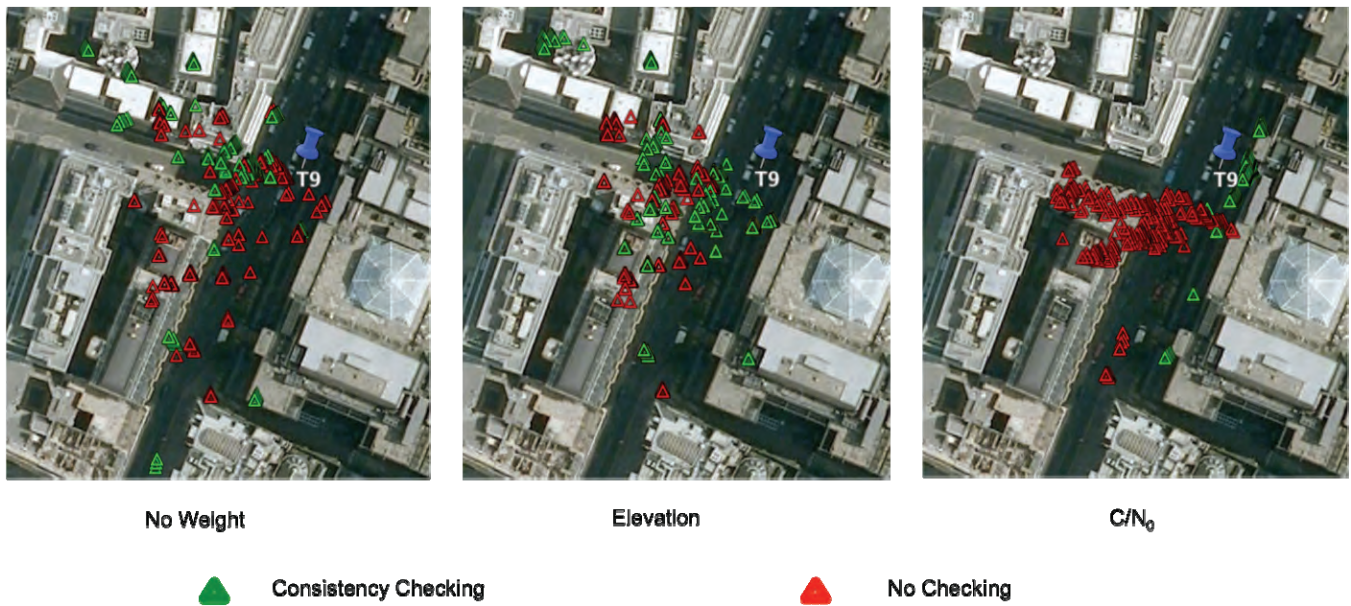


Figure 13: Error Comparison for all weighting schemes with consistency checking in Scenario 2

	No weighting	Elevation	$C/N_0$
Easting	27.9	29.45	10.29
Northing	44.58	46.38	31.32
Height	104.91	95.39	55.16

Table 4: RMS error (Meters) for all weighting schemes with consistency checking in Scenario 2

However, it is also necessary to point out the risk of the consistency checking approach. As shown in Figures 13 and 14, even for the most successful method, large positioning errors still exist. This suggests the presence of multipath contamination in the remaining signals. Because of the lack of further correction methods, this could lead to very large errors if NLOS signals are not completely excluded. Other methods that are more effective against NLOS signals are needed such as dual-polarisation antennas [3]. Further research into more advanced consistency checking methods is thus required.



**Figure 14:** Positioning results comparison for different weighting scheme with or without consistency checking in Scenario 2

### 4.3 SCENARIO 3: CAR NAVIGATION

#### Data collection

This set of data was collected across the London area in a car using a prototype GPS/GLONASS receiver designed for car navigation. The date of the data collection was 30th May 2011. The trajectory is shown in Figure 15. The journey started from South West London on the Thames riverside and circled through the central London with a combination of a moderate city environment and an extreme city canyon environment. The London City area, where the urban canyons mostly occur, was traversed repeatedly.

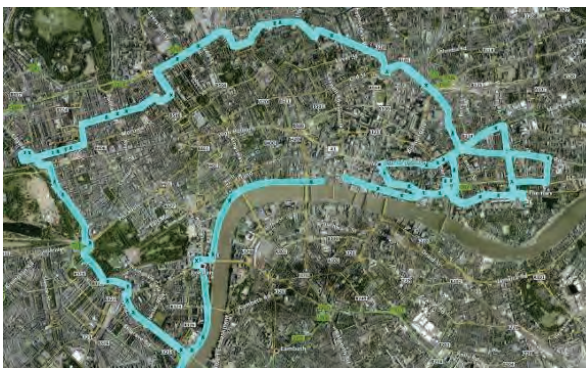


**Figure 15:** An overview of the trajectory for Scenario 3

The satellite visibility during the data collection period is shown in Figure 16. The average number of satellites available was about 15, consisting of an almost equal number from each constellation. For extreme city canyon environments, as shown between the 1st and 2nd hour in

Figure 16, a reduced number of satellites or even a complete loss of signals can be observed.

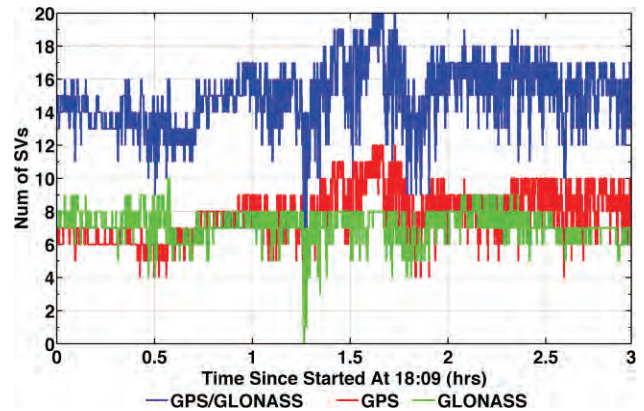


**Figure 16:** Satellite visibility during the data collection in Scenario 3

#### Applying Consistency Checking

The test was performed on algorithms both with and without consistency checking using 1-hour data from the journey covering the central London area. The  $C/N_0$ -based weighting scheme was used for both algorithms. The truth reference used here is the output from the receiver's Kalman-filter-based positioning algorithm. This filtered solution is accurate to within a few meters. The comparison of the results here is therefore relative. A comparison of the test results is shown in Figure 17.

The results in Figure 17 demonstrate both the performance improvements and the risks introduced by the consistency-checking algorithm. While the consistency checking results improves the results in



**Figure 18:** Examples of both failed and successful performance improvements in Scenario 3

general, as shown by the green dots in the figures, the risks of eliminating the wrong satellites can result in occasional large outliers in the final position solution.

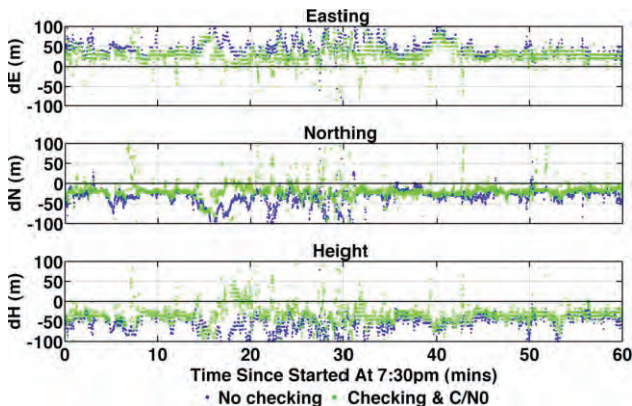


**Figure 17:** Error Comparison for solutions with/without consistency checking using  $C/N_0$  weighting in Scenario 3

Figure 18 further demonstrates the positioning performance of the algorithm with two examples, both a failure and a successful example. As can be seen in the failed example, incorrect satellites were removed, resulting in large outliers. On the other hand, successful removal of the contaminated signals significantly improves the original noisy position solutions.

## 5. CONCLUSIONS AND FUTURE WORK

This paper explored detection and mitigation of multipath and NLOS errors for dual-constellation GNSS positioning in severe urban environments using the RAIM-type consistency checking. Three types of consistency checking schemes, two weighting schemes and different ranging observables were proposed and tested.

The results show that a recursive consistency-checking method based on RAIM-type hypothesis testing improves the positioning errors under moderate multipath conditions. However, the performance is unreliable in severe environments, such as urban canyons.

One of the assumptions that this hypothesis testing approach is based on is that the signals heavily contaminated due to NLOS reception are the minority amongst the received signals. This, however, is not always true under extreme multipath and NLOS conditions, such as scenario 2 in this paper. When only a small part of sky can be seen and a large number of highly reflective objects are present at the receiver location, a set of received signals may be found that are consistent amongst themselves but still produce an erroneous position solution. Without further information on the signal or surrounding environment, the consistency-checking method struggles to work with the biased residuals.

Another assumption of the hypothesis testing is that the measurement errors follow a zero-mean Gaussian distribution; hence the core of the testing is a chi-square test examining the normality of the measurement residuals. However, as can be seen from the distribution of position solutions in this paper, errors caused by extreme multipath and NLOS signals do not become white over time. Instead, a more systematic presence is usually expected. Therefore, when only consistency checking methods are applied, it is often the precision of the solution but not the accuracy that is improved. For positioning in urban canyons, these two can be very different.

It is also demonstrated from the test results that when a suitable weighting scheme is combined with the

consistency checking methods, it is possible to improve the accuracy and reliability of the solution. Between the two proposed weighting schemes, elevation- and  $C/N_0$ -based, the  $C/N_0$ -based scheme is shown as the more effective one in the urban canyon. Although  $C/N_0$  the value of a signal tends to be correlated with its elevation in an open and moderate multipath environment, this differs significantly in an urban canyon. Heavily multipath-contaminated and NLOS signals usually exhibit a lower  $C/N_0$  value. The “clean” signals are more likely to come from the along track direction and do not necessarily have a higher elevation than other signals.

Based on the conclusions derived from the test results, the following ideas will be investigated next:

- New “bottom up” consistency checking methods will be developed that generate multiple position solutions from different 4- and 5-satellite combinations and compare them.
- For dynamic applications, time variation of the solutions residuals will be monitored as sudden changes could imply a change in multipath conditions or the reception of NLOS signals.
- Employing an adjustable test threshold for the consistency checking process to improve the robustness of the technique will be tested.

## ACKNOWLEDGMENTS

This work is part of the Innovative Navigation using new GNSS Signals with Hybridised Technologies (INSIGHT) program. INSIGHT ([www.insight-gnss.org](http://www.insight-gnss.org)) is a collaborative research project funded by the UK’s Engineering and Physical Sciences Research Council (EPSRC) to extend the applications and improve the efficiency of positioning through the exploitation of new global navigation satellite systems signals. It is being undertaken by a consortium of twelve UK university and industrial groups: Imperial College London, University College London, the University of Nottingham, the University of Westminster, EADS Astrium, Nottingham Scientific Ltd, Leica Geosystems, Ordnance Survey of Great Britain, QinetiQ, STMicroelectronics, Thales Research and Technology UK Limited, and the UK Civil Aviation Authority.

The authors would also like to thank the following people who assisted the data collection for Scenarios 1 and 2: Mr Chris Atkins, Mr Lei Wang, Mr Toby Webb and Ms Chian-yuan Li.

## REFERENCES

[1] Groves, P.D., *Principles of GNSS, inertial, and multisensor integrated navigation systems*, Artech House, 2008.

[2] Lau, L. and P. Cross, “Investigations into Phase Multipath Mitigation Techniques for High Precision

Positioning in Difficult Environments”, *Journal of Navigation*, Vol. 60. No. 4, 2008, pp. 457-482.

[3] Groves, P. D., Z. Jiang, B. Skelton, P. A. Cross, L. Lau, Y. Adane and I. Kale, “Novel Multipath Mitigation Methods using a Dual-polarization Antenna,” *Proc. ION GNSS 2010*.

[4] Feng, S., Ochieng, W.Y., Walsh, D and Ioannides, R., “A Measurement Domain Receiver Autonomous Integrity Monitoring Algorithm”. *GPS Solutions*, Springer, 10(2), (2006), 85-96.

[5] Feng, S., Ochieng, W.Y., “User Level Autonomous Integrity Monitoring for Seamless Positioning in All Conditions and Environments”, *Proceedings of the European Navigation Conference*, Manchester, 7-10, May, 2006.

[6] Mattos, P.G., *Multipath indicator to enhance RAIM and FDE in GPS/GNSS systems*, Patent Application No. 11112819.5, ST Microelectronics, Filed 26 July 2011.

[7] RTCA, *Minimum Operational Performance Standards for Global Positioning System/Wide Area Augmentation System Airborne Equipment, DO-229D*, Washington, DC, 2006.

[8] Parkinson, B.W., Spilker, J.J., Axelrad, P. and Enge, P., *Global Positioning System: Theory and Applications Volume II*, Progress in astronautics and aeronautics, 1996.

[9] Hartinger, H. and Brunner, F.K., “Variances of GPS Phase Observations: The SIGMA- $\epsilon$  Model”, *GPS Solutions*, Springer, 2(4), (1999), 35-43.

[10] Misra, P. and Enge, P., *Global Positioning System: Signals, Measurements and Performance 2nd edn.*, Lincoln, MA: Ganga-Jamuna Press, 2006.